Sensors and Materials, Vol. 16, No. 1 (2004) 001–012
MYU Tokyo

S & M 0543

Determination of Porosity Using a Water Pycnometer with Capacitive Level Detection

Vojko Matko*

University of Maribor, Faculty of Electrical Engineering and Computer Science,
Smetanova 17, 2000 Maribor, Slovenia

(Received November 7, 2002; accepted November 4, 2003)

Key words: porosity, soils, capacitive-dependent crystal, direct digital method.

In response to a need for a more accurate porosity measuring method for small solid samples (approximately 1 g in mass), the porosity measurement sensor using the sensitive capacitive-dependent crystal was developed. This paper describes the new sensor. Presented are the probe sensitivity and frequency dependence on the volume. In addition, the new idea of excitation of the entire sensor with stochastic test signals is described, and the porosity measuring method is presented. This method includes the influence of test signals on the weighting function uncertainty. The experimental results of the porosity determination in volcanic rock samples are presented. The uncertainty of the porosity measurement is less than 0.1% in the temperature range 10–30°C.

1. Introduction

Porosity is defined as the ratio of the volume of voids to the total volume of the material. Porosity in rocks originates as *primary porosity* during sedimentation or organogenesis and as *secondary porosity* at later stages of the geological development. In sedimentary rocks, the porosity is further classified as intergranular porosity between grains, intragranular or intercrystalline porosity within grains, fracture porosity caused by mechanical or chemical processes, and cavernous porosity caused by organisms or chemical processes.[1]

Rock grains are of different sizes, shapes and mineralogical composition. Among these grains we can find voids, which indicates that most rocks are porous to some degree. These voids are filled with air or water, or with air and water. Soils, too, contain pores, which can be classified as macro, meso and micro. Pore diameters larger than 0.06 mm are called macropores and those less than 0.06 mm, mesopores.[2–5] Pores in the range of 0–100

*Corresponding author, e-mail address: vojko.matko@uni-mb.si

nanometers in size are nanopores. It is well known that the properties of soils considerably depend on the distribution of pores in terms of their structure, their size, the percentage of pore volumes in relation to the total volume, the quantity of water inside them and so forth.[1,6,7]

Soils may be considered as a porous four-phase system composed of air, water, solids and admixtures. As such they can serve well to explain how porosity is estimated. In this four-phase soil system, the density ρ of soils is defined as the ratio of the sum of mass m to the sum of volume V of various soil phases:[8–11]

$$\rho = \frac{\sum m_i}{\sum V_i} = \frac{m_s + m_w + m_a + m_{ad}}{V_s + V_w + V_a + V_{ad}}, \tag{1}$$

where s is solid phase, w is water phase, a is air phase and ad is admixture. Equation (1) can also be rewritten as

$$\rho = \frac{\rho_s V_s + \rho_w V_w + \rho_a V_a + \rho_{ad} V_{ad}}{V_s + V_w + V_a + V_{ad}}. \tag{2}$$

The porosity of soil is defined by two parameters - void ratio e and porosity parameter η. The void ratio e is defined as the ratio of volume of pores to volume of particles:

$$e = \frac{V_w + V_a + V_{ad}}{V_s}. \tag{3}$$

The porosity parameter η is defined as the ratio of volume of pores to volume of soil samples:

$$\eta = \frac{V_w + V_a + V_{ad}}{V} = \frac{V_w + V_a + V_{ad}}{V_s + V_w + V_a + V_{ad}}. \tag{4}$$

In practice, we can define mass as the ratio of weight of soil to gravity:

$$m = \frac{W}{g}. \tag{5}$$

During weighting in air, the mass must be reduced due to the presence of the air:

$$m_s = \frac{W_s}{g} + \rho_a \cdot V_s, \tag{6}$$

$$m_w = \frac{W_w}{g} + \rho_a \cdot V_w , \tag{7}$$

$$m_{ad} = \frac{W_{ad}}{g} + \rho_a \cdot V_{ad} . \tag{8}$$

The degree of saturation S_r is defined as the ratio of the volume of pores saturated with water to the volume of all pores:

$$S_r = \frac{V_w}{V_w + V_a} = \frac{\eta_w}{\eta_w + \eta_a} , \tag{9}$$

where

$$\eta_w = \frac{V_w}{V} = \frac{V_w}{V_s + V_w + V_a} , \tag{10}$$

$$\eta_a = \frac{V_a}{V} = \frac{V_a}{V_s + V_w + V_a} . \tag{11}$$

1.1 *Porosity determination methods*

There are many different porosity measurement methods. The simplest one is the determination of porosity by the saturation method.[1,2] In this method, beakers are first filled to the same mark with gravel, sand, silt or a mixture of these three materials. Then water is poured into each of the beakers until it reaches the top of each material. The porosity is determined by dividing the volume of water that could be poured into the material by the total volume of that material.

$$\eta = \frac{V_{\text{void}}}{V_{\text{total}}} \cdot 100\% \tag{12}$$

Here, V_{void} is pore space volume, and V_{total} is total volume. The material used has to be consolidated to avoid the sinking of the material and edge corrections of the material have to be made. Therefore, a combination of porosity determination methods is used.

The imaging porosity method aims to identify and quantify different pore systems to determine the nature and abundance of matrix and macroporosity. Matrix porosity is characterised from digital images obtained from thin sections cut from core plugs.

Microporosity is quantified with back-scatter SEM or by a $25x$ microscope objective; larger matrix pores are quantified with $10x$ or $4x$ microscope objectives. In each digital image, the porosity is segmented by the image analysis software and a second image is created in which the porosity is picked out in false colour.[12–14]

The helium pycnometer method uses helium, which, having very small atoms, penetrates all the cracks and holes in the rock, and all the boundaries between the mineral grains, but does not penetrate the grains. The idea is to measure the pressure difference between the two containers of the pycnometer, one of which has the sample material in it. The volumes of the two chambers are known very precisely, and the difference in volumes available to the gas is due to the presence of the sample in one of the chambers. The difference in the volume of the open spaces between the two chambers is related to the difference in the pressures. The porosity of the sample is the percentage difference between the grain volume and bulk volume, divided by the bulk volume.[15]

Porosity can also be determined by other conventional methods such as the adsorption methods, mercury porosimetry, capillary methods, dielectric methods, analytical methods, proton nuclear magnetic resonance, chromatography and ultrasound methods.[16,17]

The new porosity measuring method described in this paper uses a highly sensitive sensor with reduced uncertainty of measurement results and reduced influence of disturbing noise signals.[18,19] In comparison with the helium pycnometer method it is cheaper.

Most capacitive bridge methods can be adapted to three-terminal measurements by the addition of components to balance the ground admittances.[20–22] However, the balance conditions for these and the main bridge being interdependent, the balancing process can become very tedious. Also, the signal/noise ratio is supposed to be high.

The well-known method is Miller's etalon[23] which is designed to sense small changes in the $\cong 4$ pF capacitor from the phase change of a series-resonant circuit. The weakness of Miller's etalon is a greater sensitivity to phase noise than with the bridge method, which is due to higher frequencies (up to 45 MHz).

An alternative approach has been described by Van Degrift[24] who used very sensitive tunnel-diode oscillator systems for measuring extremely small capacitance changes. This gain in sensitivity is somewhat offset by a loss in stability.

2. The Porosity Sensor

The porosity sensor uses sensitive capacitive-dependent crystals (40 MHz with stability of ±1 ppm in the temperature range from –5 to +55°C) because of their stability and long-term repeatability (Fig. 1). Two pseudo stochastic three-state signals $x_1(t)$ and $x_2(t)$ are used to influence the frequencies of the two quartz oscillators.[25–27] The frequency of oscillator 1 is 40 MHz and that of oscillator 2 is 40.001 MHz.[28,29] The output of the pulse-width modulator (EXOR) is a pulse-width signal which is compensated for temperature and voltage drift.

The sensor probe C_x is a capacitor on the outer surface of the glass test tube (Fig. 2).[30] The crystal is used as a stable oscillation element whose electrical circuit is changed through the variation of the series capacitance C_x. The values in the quartz electrical circuit and the capacitance C_x = 5 pF are measured with impedance/gain phase analyser HP 4194A.[29]

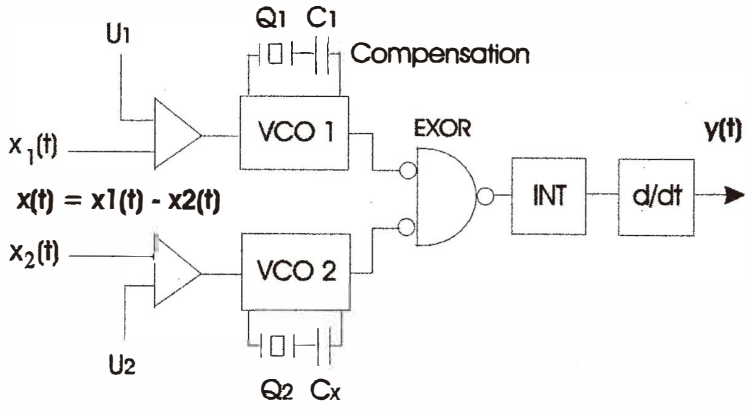

Fig. 1. Sensor structure.

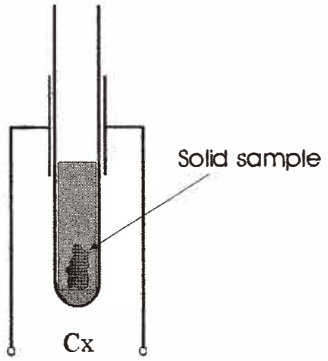

Fig. 2. Glass test tube.

The change of the liquid level causes the change of capacitance and frequency change in oscillator 2 (Fig. 1, Fig. 2). The probe dependence df on the volume is shown in Fig. 3. The frequency measurement uncertainty is ±0.1 Hz. The results suggest that the change in frequency is proportional to the volume in the 0–1 ml range.

3. Reduction of the Measurement Uncertainty

The uncertainty of the measurement results is improved by the direct digital method (DDM), which reduces the influence of disturbances.[18,19] The linear time-invariant system has been chosen due to signals $x1(t)$ and $x2(t)$, which form a special correlation function that is real-time independent.

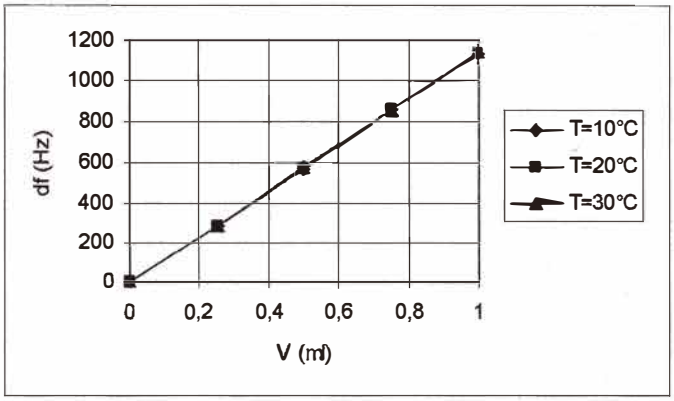

Fig. 3. Probe dependence df on the volume with signals $x1(t)$ and $x2(t)$.

$$\Phi_{xy}(\tau) = \sum_{u=0}^{T} g(u) \cdot \Phi_{xx}(\tau - u) \tag{13}$$

Here, $\Phi_{xy}(\tau)$ is the cross-collection function, $g(u)$ is the weighting function, $\Phi_{xx}(\tau - u)$ is the auto-collection function and T is the measuring period. For every value of τ, one equation with various numbers of elements is obtained. To calculate the value of the weighting functions $g(0)$, $g(1)$,...,$g(L)$ the equations are united in the system with $L + 1$ eqs. (14).

$$\begin{bmatrix} \Phi_{xy}(-P+L) \\ \cdot \\ \cdot \\ \Phi_{xy}(-1) \\ \Phi_{xy}(0) \\ \Phi_{xy}(+1) \\ \cdot \\ \cdot \\ \Phi_{xy}(M) \end{bmatrix} = \begin{bmatrix} \Phi_{xx}(-P+L) \cdots & \Phi_{xx}(-P) \\ \cdot & \cdots \\ \cdot & \cdots \\ \Phi_{xx}(-1) & \cdots \Phi_{xx}(-1-L) \\ \Phi_{xx}(0) & \Phi_{xx}(-L) \\ \Phi_{xx}(+1) & \Phi_{xx}(1-L) \\ \cdot & \cdots \\ \cdot & \cdot \\ \Phi_{xx}(M) & \Phi_{xx}(M-L) \end{bmatrix} \cdot \begin{bmatrix} g(0) \\ \cdot \\ \cdot \\ \cdot \\ \cdot \\ \cdot \\ \cdot \\ \cdot \\ g(L) \end{bmatrix}$$

$$\underline{\hat{\Phi}}_{xy} = \underline{\hat{\Phi}}_{xx} \cdot \underline{g} \tag{14}$$

The largest negative time move $\tau_{max} = -P$ and the largest positive one $\tau_{max} = M$ were used. The system of equations has thus $P - L + M + 1$ number of equations. If $M = -P + 2L$ is chosen, $L + 1$ number of equations remain, so that $\hat{\Phi}_{xx}$ becomes a square matrix and we get

$$\hat{g} = \hat{\Phi}_{xx}^{-1} \cdot \hat{\Phi}_{xy}. \tag{15}$$

If $P = L$ is determined, then the same number of values (symmetrical autocorrelation functions (AKF) because $\tau_{max} = -P = -L$ and $\tau_{max} = M = L$ for the positive and negative τ) is used to calculate $\Phi_{xx}(\tau)$. The calculation of the weighting function is simplified if the input signal is white noise with the autocorrelation function as

$$\Phi_{xx}(\tau) = \sigma_x^2 \cdot \delta(\tau) = \Phi_{xx}(0) \cdot \delta(\tau), \tag{16}$$

$$\delta(\tau)\begin{cases} 1 for \tau = 0 \\ 0 for |\tau| \neq 0 \end{cases}. \tag{17}$$

It follows that

$$\hat{g}(\tau) = \frac{1}{\hat{\Phi}_{xx}(0)} \cdot \hat{\Phi}_{xy}(\tau). \tag{18}$$

Having stated eq. (15) and having considered the measurement time t_{meas}, we get the weighting function $\hat{g}(\tau)$ as shown in eq.(18).[18,19]

4. Porosity Measurement

Due to the specially chosen test signals *x1(t)* and *x2(t)*, the function $\Phi_{xy1}(\tau)$ begins at the origin of coordinates and ends on the X axis when $\tau = t_{meas}$ (Fig. 4). Consequently, the porosity is defined as a change of area (surface) between the functions $\Phi_{xy2}(\tau)$ and $\Phi_{xy1}(\tau)$, whose change is defined by capacitance *Cx*. In this way, the test signal has been considered throughout the entire t_{meas} period, as well as the sign change compensation in the calculation of the cross-correlation function. Compared with the measurements that are not DDM-method based, the improvement of the signal/noise ratio by ≅ 30 dB is the most significant gain.

The frequency is simultaneously converted into volume units by calibrating the ratio between the frequency and the volume for each glass tube. Mercury, whose mass is measured at an error of 0.01% (at known temperature) is used for calibration.[31] The mechanical nonlinearities of the glass tube which, according to the producer's data, do not exceed 0.01%, are taken into account. The dependence can be linearized by using the spline method.

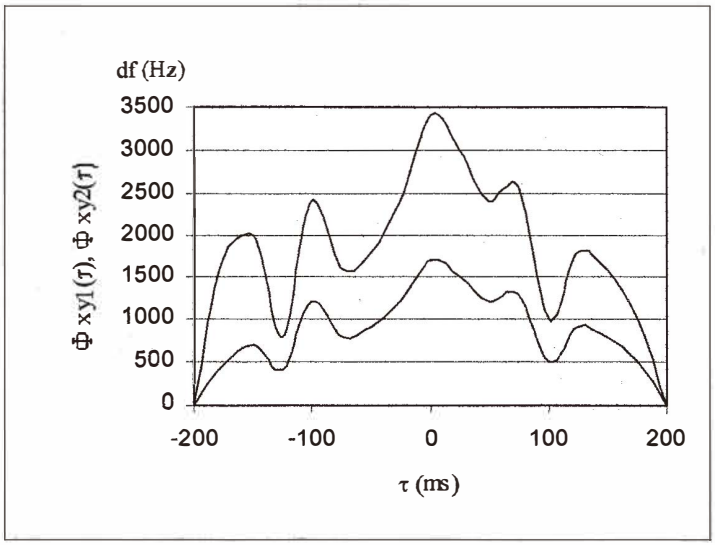

Fig. 4. Functions.

The influence of temperature on measurements is considered in three ways. We must know the influence of the temperature on the measurement equipment, on the measurement medium in which the measurement is performed (i.e., the fluid in which the test is carried out), and the influence of the rock temperature on its physical properties.[31]

The temperature of the environment affects the linearity of the measuring sensor. Calibration is used to establish the measurement error of the sensor which is 0.03%. If the relation between the output frequency and the volume is known (Fig. 3), we get

$$V(T) = V(T_0) + \Delta V(T). \tag{19}$$

Equation (19) gives the correction of the measurement with respect to temperature changes. Temperature changes also affect the volume of the measurement medium, i.e., of the rock sample. Consequently, the change of volume due to temperature changes is expressed in the determination of the rock's specific gravity as follows

$$\gamma(T) = \gamma(T_0) + \Delta\gamma(T). \tag{20}$$

Under the conditions of a linear temperature relationship inside a certain temperature range, it holds true that

$$V(T) = V_s(T_0) \cdot \left(1 + \alpha_{V_s}\left(T - T_0\right)\right). \tag{21}$$

The change of volume due to temperature changes in naturally humid soils is expressed as the sum of volume changes of all rock phases:

$$dV(T) = dV_s(T) + dV_w(T) + dV_a(T). \tag{22}$$

The total measurement error of the porosity sensor in relation to individual partial influences such as glass tube nonlinearity, calibration with mercury, the influence of temperature on the sensor (Fig. 3), linearization of df on V, frequency measurement $y(t)$ (Fig. 1), specific rock weight, change of water volume in the test tube and the change of sample volume $dV(T)$ in eq. (22) is 0.1% (10–30°C).

5. Experimental Porosity Measurement

To test the new method, volcanic rock samples, which are known for their porosity, were selected for experimental determination of porosity. Four characteristic samples approximately 1 ml in size and 1 g in weight were gathered near Puerto de Santiago, Mount Teide (3715 m), Tenerife.

All test samples were randomly selected. To determine the porosity of a random solid sample (at 20°C), the latter is immersed in water contained in a test tube around which the capacitor C_x is placed (Fig. 2). The volume of the sample is measured. In the first case, the glass solid sample with 0 % porosity was immersed (Fig. 5). The frequency did not change, which indicates that there was no air leak. In the second case, a dry randomly selected volcanic rock sample (weighting 0.821 g) was immersed in the water. Since the sample was porous, the air leaked, which was reflected in the dynamic change of frequency (Fig. 6). The transitional phenomenon caused by immersion ends in 1 ms.[32] The measurement is performed until the final state towards which the measurement limit is reliably predicted

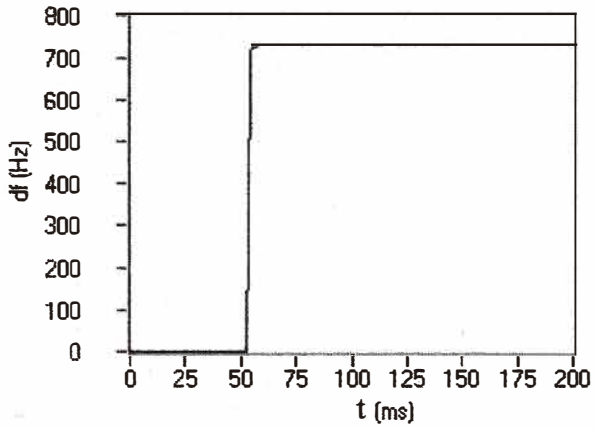

Fig. 5. Measurement of sample having 0% porosity.

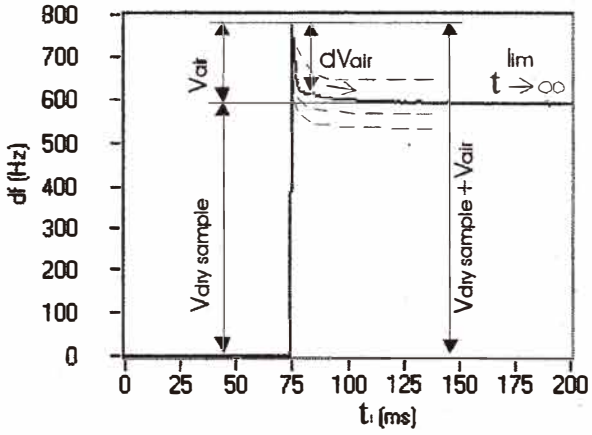

Fig. 6. Air leak after sample immersion.

(the capillary effect is taken into account). Depending on the degree of porosity, this saturation limit is higher or lower as shown for the other three samples (Fig. 6). At a known temperature the sample porosity can be determined.

$$\eta = \frac{V_{air}}{V_{dry\ \ sample} + V_{air}} \tag{23}$$

The sample porosity in Fig. 6 was 23.8%. Taking into account total measurement error, which is 0.1% in the temperature range 10–30°C, we can conclude that the measurement is ±1% accurate. To evaluate the accuracy of this method, this result should be compared to mercury porosimetry and helium pycnometry. The fastest measurement time without test signals is 1 μs. These measurement results show the applicability of the new method, which in combination with other porosity determination methods such as weighing methods, helium pycnometry, powder pycnometry and mercury pycnometry, could serve as a quality control procedure.

6. Conclusion

The porosity sensor using the capacitive-dependent crystals has been described and the dependence of *df* on the volume of the sensor probe has been presented. In addition, the porosity measurement method has been given. The latter includes the influence of test signals on the weighting function uncertainty.

The formation of the cross-correlation function between the test signal $x(t)$ and the system response $y(t)$ decreases the influence of all disturbing signals that are not correlated

to the test signal $x(t)$ for ≅ 30 dB.[18,19] Other advantages of the proposed method are high sensitivity, high stability, a series resonant circuit which is not composed of the elements L and C, the signal/noise ratio does not affect the accuracy of measurements, reduced disturbances due to the structure and the method, the long-term repetition, reduced hysteresis[28] and low cost. It should be noted, however, that pairs of crystals with similar temperature characteristics should be used. The accuracy and repeatability are determined only from the temperature frequency difference of the crystal pairs.[33]

Experimental results confirm the applicability of the porosity sensor. The sensor using quartz crystals enables very accurate measurements for consolidated materials provided that edge corrections are made. The subsequent computer analysis and statistical processing of obtained results additionally reduce the measurement error. The sensor was used in rheological research using compressed soil samples. In addition to high-quality interpretation of results, this method also offers immediate on-site interpretation, if the specific gravity is known. Furthermore, the measurements can be performed on a large number of small samples of any shape which allows the establishment of the local heterogeneity of the material.

References

1 J. Schoper: Physikalische Eigenschaften der Gesteine **V/Ia** (1982) 184.
2 A. Netto: Bull. Appl. Math. **77** (1993) 1101.
3 P. Sheng: Phys. Rev. B. **41** (1993) 4507.
4 J. Howard and W. Kenyon: Marine and Petroleum Geology **9** (1992) 139.
5 S. Sakai: Journal of Membrane Science **96** (1994) 91.
6 P. Doyen: J. Geophys. Res. **93** (1988) 7729.
7 J. Harlan, D. Picot, and P. Loll: Analytical Biochemistry **224** (1995) 577.
8 M. Spearing and P. Matthews: Transport in Porous Media **6** (1991) 71.
9 G. Matthews and M. Spearing: Marine and Petroleum Geology **9** (1992) 146.
10 M. Kwiecen, I. MacDonald and F. Dullien: J. Microsc. **159** (1990) 343.
11 K. Meyer, P. Lorenz, B. Böhl-Kuhn and P. Klobes: Cryst. Res. Techn. **29** (1994) 903.
12 J. Berryman: J. Appl. Phys. **57** (1985) 2374.
13 W. W. Chen and B. Dunn: Journal of the American Ceramic Society **76** (1993) 2086.
14 J. Fredrich, B. Menendez and T. Wong: Science **268** (1995) 276.
15 H. Franz: Feinwerktechnik & Meβtechnik **95** (1987) 145.
16 J. Fripiat: Porosity and Adsorption Isotherms, Fractal Approach to Heterogeneous Chemistry, Wiley (1989) p. 28.
17 G. P. P. Gunarathne and K. Christidis: Measurements of Surface Texture Using Ultrasound, IEEE Trans. Instrum. Meas., 50 (5), October (2002) p. 1144.
18 K. W. Bonfig: Das Direkte Digitale Messverfahren (DDM) als Grundlage einfacher und dennoch genauer und störsicherer Sensoren, Sensor Nov. (1988) s. 223.
19 V. Matko and J. Koprivnikar: Measurement of 0-1 ml Volumes Using the Procedure of Capacitive - dependent Crystals, IEEE Trans. Instrum. Meas., 43 (3), Jun. (1994) p. 436.
20 M. C. McGregor, J. F. Hersh, R. D. Cutkosky, F. K. Harris, and F.R.Kotter: New Apparatus at the National Bureau of Standards for Absolute Capacitance Measurement, IRE Trans. Instr. 1–7 (3-4) (1958) p. 253.
21 A. M. Thompson: IRE Trans. Instr. **1–7**(1958) 245.
22 C. Moon and C. M. Sparks: J.Res. NBS **41** (1948) 497.

23 G. L. Miller and E. R. Wagner: Rev. Sci. Instrum. **61** (1990) 1267.
24 C. T. Van Degrift: Rev. Sci .Instrum. **52** (1981) 712.
25 E. Bartels and T. Funk: J. Phys. E. **16** (1983) 1105.
26 K. Dmowski: Rev. Sci. Instrum. **61** (1990) 1319.
27 M. Bertocco, A. Flammini, D. Marioli and A. Taroni: Fast and Robust Estimation of Resonant Sensors Signal Frequency, IEEE Trans. Instrum. Meas., 51 (2), April (2002) p. 326.
28 V. Matko and J. Koprivnikar: Capacitive Sensor for Water absorption Measurement in Glass-fiber Resins using Quartz Crystals, IAAMSAD:South African branch of the Academy of Nonlinear Sciences, Proceedings, Durban, South Africa (1998) p. 440.
29 V. Matko and J. Koprivnikar: Quartz Sensor for Water Absorption Measurement in Glass-fiber Resins, IEEE Trans. Instrum. Meas., 47 (5), Oct. (1998) p. 1159.
30 M. Stucchi and K. Maex: Frequency Dependence in Interline Capacitance Measurements, IEEE Trans. Instrum. Meas., 51 (3), Jun. (2002) p. 537.
31 R. C. Weast: CRC Handbook of Chemistry and Physic, 67th edition, Boca Raton, Florida (1987) p. E49–E52.
32 P. Gennes: Wetting: Rev.Mod.Phys. **57** (1985) 827.
33 J. Fraden: American Institute of Physics (1997) ISBN 1-56396-538-0.